J. Eur. Opt. Society-Rapid Publ. 2025, **21**, 25
© The Author(s), published by EDP Sciences, 2025
https://doi.org/10.1051/jeos/2025023
Available online at: https://jeos.edpsciences.org

EOSAM 2024
Guest editors: Luca De Stefano and Raffaele Velotta

Journal of the European Optical Society-Rapid Publications

REVIEW ARTICLE

OPEN ACCESS

Backward-wave optical parametric oscillators: principles, applications, and recent advancements

Fredrik Laurell* and Valdas Pasiskevicius

Department of Applied Physics, Royal Institute of Technology, Hannes Alfvéns väg 12, 11419 Stockholm, Sweden

Received 5 February 2025 / Accepted 29 April 2025

Abstract. Backward-wave optical parametric oscillators (BWOPOs) represent a significant advancement in nonlinear optics, offering unique capabilities such as narrowband, highly stable outputs without the need for mirrors or coatings. Leveraging self-established distributed feedback, these devices exhibit exceptional spectral and spatial properties. This paper explores the principles behind BWOPOs, materials and techniques used, and their applications, particularly in mid-infrared lidar systems including CO_2 monitoring. Recent developments in cascaded systems and BWOPO waveguides are highlighted, demonstrating the potential of BWOPOs to revolutionize laser technology.

Keywords: Nonlinear optics, backward-wave optical parametric oscillation, Laser, Gas sensing.

1 Introduction

Optical parametric oscillators (OPOs) are versatile and widely used sources of tunable coherent light and constitutes a crucial part of nonlinear optics [1]. They rely on the process of optical parametric amplification (OPA), where a nonlinear crystal mediates the conversion of a high-energy photon from a pump beam into two lower-energy photons, the signal and idler. Conventional OPOs consist of a nonlinear crystal, enclosed in a cavity for radiation buildup. They operate in a forward configuration, where the signal and idler waves are generated colinearly with the pump beam. For efficient energy transfer the phase-matching condition must be fulfilled as the signal and idler waves travel forward along with the pump beam throughout the nonlinear crystal. The parametric process conserves energy and momentum, and by tuning the latter output is possible across a wide range of wavelengths, from the ultraviolet to the mid-IR. Originally birefringent phase-matching was exploited, where tuning was obtained either by adjusting the temperature of the sample, by rotating it, or by tuning the pump wavelength. Today quasi-phase matching (QPM) is the most commonly used technique to obtain tuning. Here a periodic modulation of the nonlinearity adds to the phasematching condition and allow flexibility in generation of desired wavelengths. OPOs play a significant role in spectroscopy, quantum optics, laser sources, and telecommunications due to their flexibility in generating light at wavelengths not easily accessible by traditional lasers [2, 3].

The development of OPOs traces back to the early 1960s, shortly after the advent of the laser in 1960. The theoretical foundation for parametric processes in nonlinear optics was laid by Bloembergen and his colleagues [4], while the first experimental demonstration of an OPO came in 1965, when Giordmaine and Miller successfully generated tunable coherent light using a lithium niobate crystal pumped by a ruby laser [5]. The same year a Russian group led by Khokhlov also demonstrated an OPO [6]. These marked pivotal moments, showcasing the potential of nonlinear optics to generate wavelengths not readily accessible with conventional lasers. Over the years, OPOs became increasingly important due to the tunability of the phase matching condition within nonlinear crystals, enabling efficient conversion of pump photons into signal and idler photons.

The concept of backward-wave optical parametric oscillators (BWOPOs) emerged as an extension of OPO research and inspiration from backward microwave oscillators (carcinotrons) [7]. The backward-wave process, in which the signal and/or idler photon propagates in the opposite direction to the pump photon, was theoretical proposed in 1966 [8]. However, it was not until the late 1990s and early 2000s that significant experimental and theoretical breakthroughs occurred [9, 10]. The backward interaction has a tough phase-matching condition which requires QPM and a very densely modulated χ^2 nonlinearity. This configuration leads to distinct properties, such as enhanced spatial coherence and high beam quality. Additionally,

* Corresponding author: flaurell@kth.se

a consequence of the single-pass configuration BWOPOs does not suffer from back-conversion and can hence provide improved energy conversion efficiency. These features make BWOPOs a promising avenue for generating high-quality, tunable light in specialized applications, particularly where narrow linewidths or precise control over spatial beam characteristics are necessary.

This paper is structured as follows: First, we provide background on nonlinear optics with a focus on QPM, followed by a discussion of the fundamental principles of BWOPOs. We then present specific examples of BWOPO configurations, including cascaded BWOPOs, phase-locked degenerate BWOPOs, and BWOPOs implemented in waveguides. Applications of BWOPOs are subsequently explored, with particular emphasis on gas sensing and CO_2 monitoring. The paper concludes with a summary and an outlook on future research directions.

2 Background on nonlinear optics using QPM towards the backward-wave optical parametric oscillator

Nonlinear optics involves the interaction of light with matter to produce new frequencies or amplify existing signals. Three-wave mixing processes, governed by energy conservation ($\omega_1 + \omega_2 = \omega_3$), are fundamental to devices like OPOs. QPM allows engineers to optimize these interactions by tailoring the periodicity of nonlinear materials, enabling efficient energy transfer while maintaining phase coherence [4]. The phase mismatch between interacting waves is in QPM compensated by periodically reversing the sign of the nonlinear coefficient of the material. This periodic modulation allows the waves to remain in phase over longer distances, enhancing the energy transfer.

Efficient energy transfer requires phase-matching and for QPM the condition can be expressed as,

$$k_1 = k_2 + k_3 + K_g, \tag{1}$$

where k_i are the are the wavevectors of the interacting waves and K_g is the grating vector, defined as,

$$K_g = \frac{2\pi m}{\Lambda}, \tag{2}$$

describing the periodic modulation of the nonlinear coefficient. Λ is the grating vector imposed by periodic poling of the nonlinear medium and m is the order parameter. When one of the generated waves is to be traveling in the opposite direction to the driving pump wave, as in the case of the BWOPO, the phase-matching condition becomes.

$$k_p = k_f - k_b + K_g. \tag{3}$$

where the subscripts p, f, and b denote pump wave, forward wave, and backward wave, respectively. The grating vector $K_g = \frac{2\pi m}{\Lambda}$, then becomes very large as can be seen in Figure 1a. The grating period becomes correspondingly small, in most cases in the sub-μm range, and in the order of half of the wavelength of the counterpropagating wave.

The field of QPM nonlinear optics took off with the demonstration of domain engineered lithium niobate and $KTiOPO_4$ (KTP) waveguides in 1989 [11–14]. It led forward to the development of electric field poling allowing QPM to be realized in bulk samples [15, 16]. Today this technology is well-established and periodically poled lithium niobate (PPLN) and periodically poled KTP (PPKTP) are commercially available from several vendors and used in many products.

PPKTP and periodically poled Rubidium doped KTP (PPRKTP) are two materials that have been widely used in nonlinear optics. They are thermally stable and show high damage thresholds and can hence operate under high-intensity conditions, which is crucial for BWOPOs. PPKTP and PPRKTP are also less susceptible to photorefractive damage, blue and green induced IR absorption than for example PPLN [17, 18]. Additional important properties of crystals from the KTP family are their wide transparency range (roughly 350–4500 nm) and their high nonlinear optical coefficients [19, 20].

So far, the only materials in which BWOPOs have been demonstrated are PPKTP and PPRKTP. This falls back on the material's quasi-one-dimensional crystal structure which enables fabrication of the dense domain gratings required for backward processes. The technology for making dense domain gratings was developed by Zukauskas et al. [21, 22] and is based on fabrication of a coercive field grating by ion-exchange followed by electric field poling. This has enabled fabrication of gratings with periods as short as 317 nm in 1 mm thick PPRKTP [23]. It corresponds to a domain aspect ratio of 6000:1 (height/width) and 60,000 domains in a 10 mm long sample.

3 Principles of the backward-wave optical parametric oscillator

The BWOPO differs from the conventional copropagating OPO by generating photons counterpropagating to the pump. This geometry relies on self-established distributed feedback where no external cavity is needed to build up the parametric waves. As no cavity mirrors are needed the device has also been referred to as a mirrorless optical parametric oscillator or MOPO [8]. Harris was the first to devise a BWOPO in 1966 [9], and the first demonstration was done by Canalias and Pasiskevicius in 2007 [8]. A BWOPO setup can be very simple and compact with just a pump laser and basic optics, as can be seen in Figure 2.

The frequency dependence of the forward and backward waves is obtained by differentiating equation (1) with respect to the pump frequency, v_p:

$$\frac{1}{v_p} = \frac{\partial k_f}{\partial \omega_p} - \frac{\partial k_b}{\partial \omega_p}, \tag{4}$$

which can be transformed to the following two expressions,

$$\frac{\partial \omega_f}{\partial \omega_p} = \frac{v_{gf}(v_{gb} + v_{gp})}{v_{gp}(v_{gb} + v_{gf})} \equiv 1 + \varepsilon, \tag{5}$$

$$\frac{\partial \omega_b}{\partial \omega_p} = \frac{v_{gb}(v_{gp} - v_{gf})}{v_{gp}(v_{gb} + v_{gf})} \equiv -\varepsilon, \tag{6}$$

with the group velocity $v_g \equiv \frac{\partial \omega}{\partial k}$. It can be seen in equation (6) that the dimensionless parameter ε is proportional to the group velocity difference between the forward and the backward wave. When the BWOPO operates far from resonance and in the low dispersion regime it implies that $|\varepsilon| \ll 1$. Consequently, the wavelength of the forward wave tunes with the pump frequency and the backward wavelength becomes almost insensitive to the pump frequency, as illustrated in Figure 1b. In the case of broadband multi-longitudinal pump, the forward wave spectrum becomes broadband, while the backward wave stays narrow.

Similar to a conventional OPO, the BWOPO exhibits an oscillation threshold. As it is rather high the experimentally demonstrated BWOPOs have been based on pulsed pump lasers [24], while CW operation is still to be demonstrated [25]. As the backward wave interacts with the pump inside the crystal in a single pass it is beneficial if the pump pulse duration Δt_p is longer than the time it takes the pump to travel to the end of the crystal, and the backward wave back to the entrance,

$$\Delta t_p \geq L\left(\frac{1}{v_{gp}} + \frac{1}{v_{gb}}\right). \tag{7}$$

It is possible to use shorter pulses, but the efficiency is then drastically reduced. Godard et al. [26] have developed an analytical model for the threshold under pulsed and CW operation. The latter can be written,

$$I_{th}^{\mathrm{CW}} = \frac{\varepsilon_0 c n_b n_f n_p \lambda_b \lambda_f}{32 d_{\mathrm{eff}}^2 L^2}. \tag{8}$$

where n_b, n_f, and n_p are the refractive indices for the backward, forward and pump wave, respectively. λ_b and λ_f are the backward and forward wavelengths and d_{eff} and L are the effective nonlinearity and sample length, respectively.

An example of how the energy and spectrum is transferred from the pump to the signal and idler for a BWOPO is shown in Figure 3. A PPKTP sample with 800 nm grating period was pumped with 480 ps stretched pulses from a regeneratively amplified Ti:sapphire laser. The pump was centered at 814.5 nm and had a frequency bandwidth of 1.21 THz. The forward wave (signal) had a central wavelength of 1123 nm and a FWMH spectral width of 410 GHz, while the backward wave is centered at 2952 nm with a narrow linewidth of only 13 GHz. One can also see how the spectrum is depleted at the longer wavelength of the pump pulse, which is then mirrored for the signal [27].

With Q-switched nanosecond pulses it is possible to obtain high pulse energies. Liljestrand et al. demonstrated a BWOPO in PPRKTP pumped at 1064 nm [28]. It had a forward propagating signal at 1740 nm and a counter-propagating idler at 2741 nm, with mJ outputs for both beams and a total signal-and-idler conversion efficiency of 47%, see Figure 4a. Both generated waves had narrow spectral bandwidths, thanks to the unique properties of the counter-propagating nonlinear interaction and the single frequency pump laser. Liljestrand compared the spectrum of the backward wave with a regular singly resonant OPO (SRO) designed for the same wavelength and measured an almost 100-fold reduction in linewidth (see Fig. 4b).

As can be seen in Figure 4 there is no role-off in the conversion efficiency curve for the BWOPO. This means that there is no back-conversion, which is a consequence of the single pass configuration and promise that the conversion efficiency can be scaled further. Mølster et al. recently demonstrated a BWOPO with more than 70% conversion efficiency at high repetition rate, using a diode laser seeded Yb-amplifier system [29]. This system was built as a prototype for atmospheric greenhouse gas monitoring, and it could be tuned with the seed laser on-off the absorption lines of carbon dioxide.

For certain applications, like long distance LIDAR sensing, further energy scaling might still be necessary. To evaluate this, a BWOPO was combined with a three-stage optical parametric amplifier using a single pump laser, see Figure 5. The pump was a single-longitudinal mode, injection seeded, 100 Hz, 10.5 ns, Q-switched diode-pumped Nd:YAG laser power amplifier system operating at 1064 nm with a maximum output energy of 110 mJ. The pump beam was split in two, where the weaker part pumped the BWOPO and the remaining pump was sent to the three-stage amplifier section to boost the output energy. Energies exceeding 20 mJ per pulse was obtained, while maintaining the narrow linewidth and high stability of the BWOPO [30]. As the OPA crystals had broad bandwidth the output could in this figuration be easily tuned just by changing the temperature of the BWOPO crystal.

3.1 Cascaded BWOPOs

When a BWOPO is pumped hard the generated signal can become strong enough to act as the pump for consecutive BWOPOs. This cascade effect enables the generation of additional signals and idlers in a stepwise manner. The energy condition for the first BWOPO is given as:

$$\omega_{p1} = \omega_{s1} + \omega_{i1}, \tag{9}$$

where the ω_{p1}, ω_{s1}, and ω_{i1} are the pump, first signal (forward) and first idler (backward) frequencies. ω_{s1} then becomes the pump generating a second signal and idler as;

$$\omega_{s1} = \omega_{p2} = \omega_{s2} + \omega_{i2}. \tag{10}$$

The corresponding phase-matching conditions are:

$$k_p = k_{s1} - k_{i1} + K_g \tag{11}$$

and

$$k_{s1} = k_{s2} - k_{i2} + K_g. \tag{12}$$

With strong enough pumping the second signal can then even drive a third BWOPO.

An example of such a cascaded BWOPO used a PPRKTP sample with a period 755 nm which was pumped with 240 ps pulses at 800 nm [31]. It generated a first signal at 1125 nm and an idler at 2763 nm. With further pumping

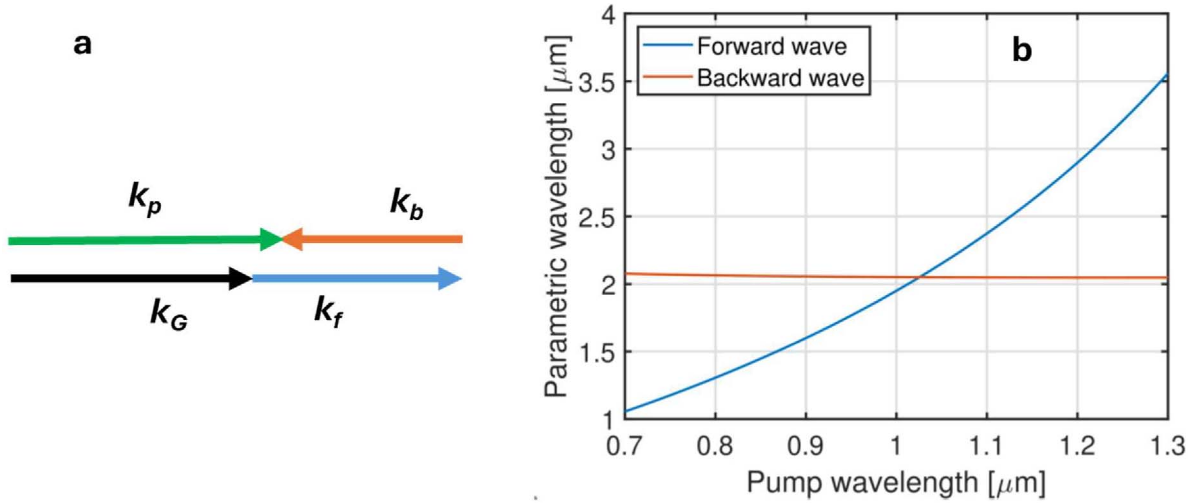

Fig. 1. a) Wavevector diagram for a BWOPO. b) Calculation of forward and backward wavelengths as a function of the pump wavelength for a PPKTP BWOPO with a grating period of 433 nm.

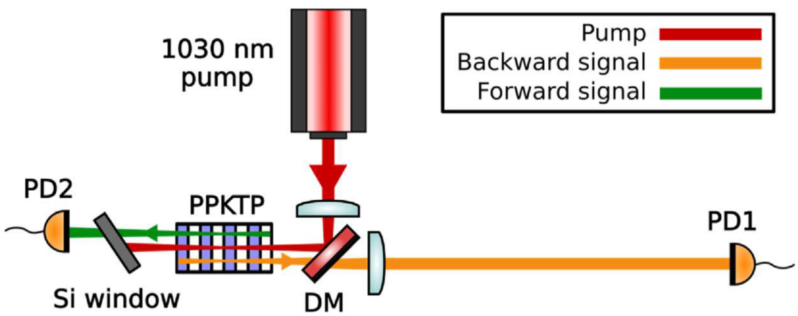

Fig. 2. Sketch of a BWOPO where the laser is focused and folded with a dichroic mirror (DM) into the nonlinear crystal,PPKTP in this case, and the backward and forward beams are measured at the two detectors PD1 and PD2. The Si window absorbs remaining pump while transmitting the forward wave.

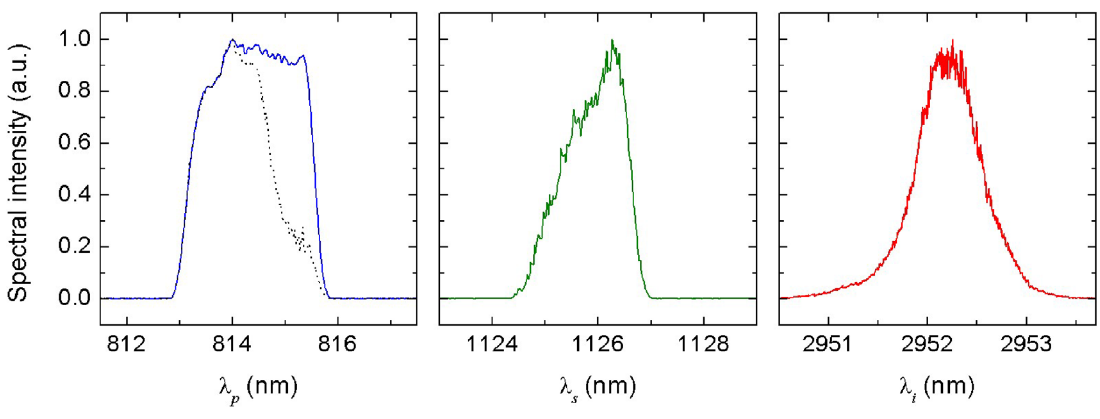

Fig. 3. Spectra for a ps BWOPO. Undepleted (solid line) and depleted (dashed line) pump (left), forward wave (middle), and backward wave (right). The FWHM widths of the pump and signal were 1.21 THz and 410 GHz, respectively, while the deconvoluted idler was 13 GHz (FWHM) [27].

the signal generated a second BWOPO where the signal appeared at 1898 nm and the idler 2739 nm. With yet stronger pumping this second signal could drive a third BWOPO with the signal at 2762 nm and the idler at approximately 5900 nm.

3.2 Phase-locked degenerate BWOPOs

Mutter et al. demonstrated the first degenerate BWOPO, meaning that the forward and backward wave had the same frequency [32]. This was done by pumping a 7 mm long

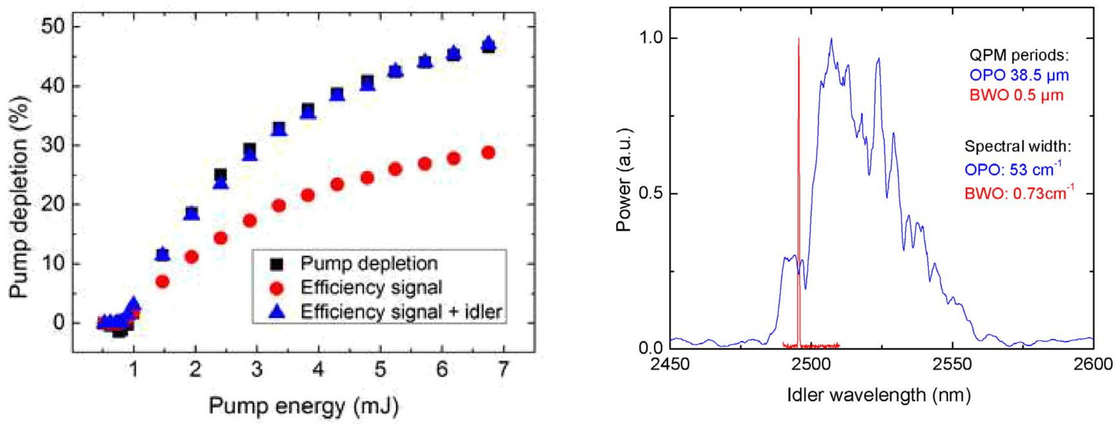

Fig. 4. Conversion efficiency for a ns BWOPO (left) and spectrum for the BWOPO (red) compared with an SRO (blue) pumped with the same laser (right) [28].

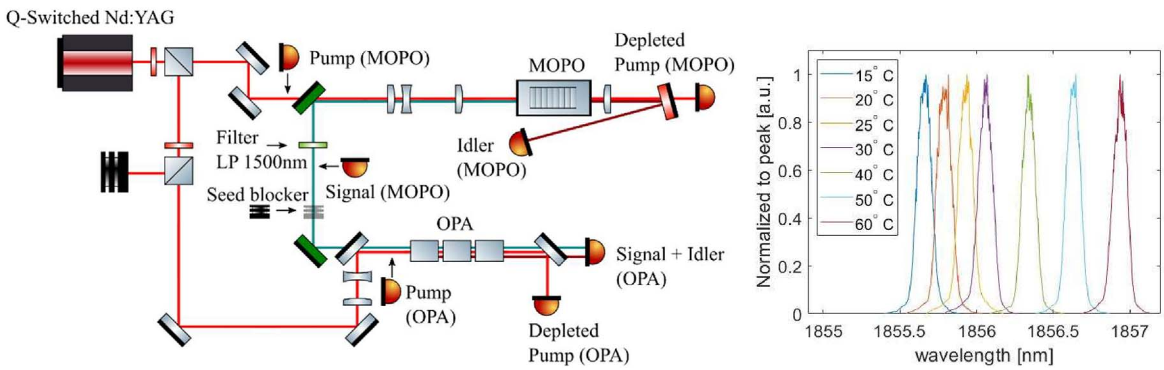

Fig. 5. Sketch of the BWOPO amplifier setup (left). It was pumped with 8 ns pulses at 1064 nm. Part of the pump beam was used to pump the PPKTP OPA crystals. The backward beam had a bandwidth of 274 MHz at 1856 nm and was tunable with temperature of the BWOPO crystal, as seen in the graph to the right [30].

PPRKTP sample with a QPM period of 455 nm with stretched pulses from a Ti:Sapphire regenerative amplifier.

The BWOPO reached degeneracy when pumped at 798.35 nm and the parametric outputs were centered at a wavelength of 1596.7 nm for both forward and backward waves. At a pump energy of 20.5 μJ, a pump depletion of 47.3% was measured with a conversion efficiency into the backward and forward waves of 40.7%. An interesting feature was that the signal and idler phase-locked stably at the degeneracy point. It was verified by doing an interference measurement between the two beams [32].

3.3 BWOPO in waveguides

The first waveguide based BWOPO was recently demonstrated and leveraged the benefits of waveguide technology to enhance nonlinear optical interactions [33]. By confining light within a small cross-sectional area, the waveguide maintains a high optical intensity over a long length, enabling efficient parametric oscillation at significantly lower pump power compared to bulk systems. Waveguides was for this purpose fabricated on the polar surface of a 20 mm long RKTP crystal utilizing a two-step process. Initially, a segmented ion-exchanged periodic structure was formed, serving as waveguides and a coercive field grating. Subsequently, the QPM grating was inscribed via electric field poling. A Ti:Sapphire regenerative amplifier was used as the pump source, providing linearly chirped pulses with a duration of 215 ps at a repetition rate of 1 kHz. The pulses had a centre wavelength of 798.9 nm and a spectral bandwidth of 470 GHz. The light was coupled into the waveguides through an objective lens with a numerical aperture of 0.28, and a low loss of 0.2 dB/cm was measured, similar to the lowest values achieved for KTP waveguides [34, 35]. The backward wave was generated at 1515 nm and the forward wave at 1689 nm. The lowest oscillation threshold was 325 nJ obtained for a 9.8 μm wide waveguide, see Figure 6, which was 19 times lower than what was obtained in the bulk of the same sample. At a pump energy of 714 nJ, a peak conversion efficiency of 8.4% was observed, while it declined at larger pump energies due to the emergence of backward stimulated polariton scattering (BSPS) [36].

4 Applications

The unique properties of the BWOPO can be exploited in many different applications where narrow linewidth and stable coherent radiation is required. The possibility for fine tuning provides additional advantages of this new device.

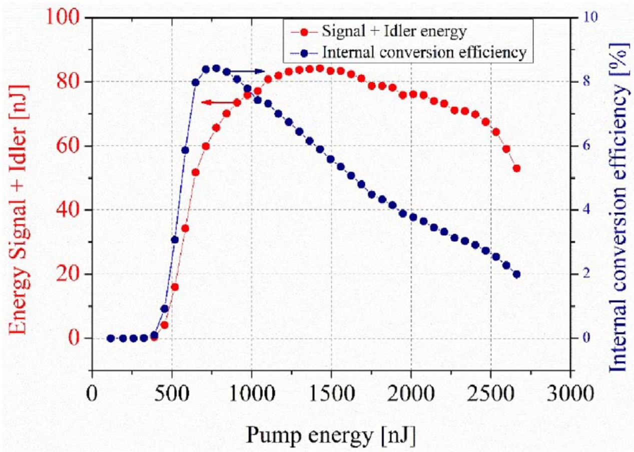

Fig. 6. Internal conversion efficiency and energy of the parametric waves as a function of the pump energy. The roll-off in conversion efficiency is due to generation of BSPS [36].

In telecommunications, precise wavelength control is necessary for dense wavelength division multiplexing where the BWOPO can be used as a reference laser [37]. Also, coherent communication relies on precise phase and frequency control of the optical signal which requires a reference laser [38]. The insensitivity to environmental disturbance would make the BWOPO ideal as a local oscillator laser in these systems.

In quantum technologies, ultra-stable light sources are indispensable for manipulating qubits in quantum computing, generating entangled photons for secure quantum communication, and powering ultra-precise optical atomic clocks. Spontaneous parametric down-conversion (SPDC) in nonlinear crystals is the workhorse of quantum optics because of its reliable ability to generate entangled photons and squeezed states of light. The automatic separation of the down-converted photons in the case of a BWOPO provides a pathway for generating high-purity and narrowband heralded single photons [39–41]. It can pave the way for efficient biphoton sources but also serve as simple and robust generators of squeezed states, hence providing a novel component for applications in optical quantum networks, quantum sensing, and related fields. The unique phase-matching conditions of BWOPOs also allow for efficient and coherent generation of quantum states of light, contributing to advancements in fields like quantum cryptography and quantum metrology.

The BWOPO can also find biomedical applications including improved imaging resolution in optical coherence tomography (OCT), enhancing sensitivity in Raman spectroscopy, and targeting specific wavelengths in photodynamic therapy. The ability to generate coherent radiation across a wide range of wavelengths with exceptional spectral purity making them ideal for precision analysis of atomic and molecular transitions. This has applications in remote sensing where BWOPOs will be valuable for probing molecular structures with high spatial and spectral resolution, particularly in the near to mid-infrared region where many molecules have strong absorption features. We hence foresee that the BWOPO will play a critical role in gas sensing for environmental monitoring.

4.1 Applications of BWOPOs in gas sensing

Mid-IR lidar systems directly benefit from the exceptional spectral properties of BWOPOs, allowing precise measurements of atmospheric components. The narrowband, tunable output of PPKTP BWOPOs is ideal for enabling single or multi-species detection with high resolution. In addition to CO_2 monitoring, BWOPOs hold promise for detecting other trace gases, such as methane, ozone, and nitrous oxide, which are pivotal in understanding anthropogenic impacts on the environment.

An important feature of the BWOPO for gas sensing is the possibility to choose wavelength band throughout the mid-IR region by addressing absorption lines with low or high absorption cross sections depending on measurement distance. This enables high detection sensitivity even in low-concentration scenarios. Additionally, the resilience to damage of PPKTP [42, 43], the high energy efficiency and the small footprint makes the BWOPO well suited for spaceborne platforms. These characteristics ensure reliable performance in harsh environments, such as outer space or high-altitude operations, where traditional systems may falter. The compact and portable design will also be important in deployment for real-time gas monitoring in industrial, environmental, or medical settings, and the stability and robustness of BWOPOs make them well-suited for continuous and long-term CO_2 monitoring under varying environmental conditions.

4.1.1 CO_2 monitoring

A first demonstration of BWOPO gas sensing was done by Vågberg et al. who exploited the backward wave's narrow linewidth and stability to accurately detect ambient CO_2 at the strong absorption lines at 2.7 μm [44]. This verified the BWOPO capability and the potential for atmospheric studies and climate monitoring. The simple experimental configuration seen in Figure 2 was used. The pump laser was a multi-longitudinal mode, Q-switched micro-chip laser with a wavelength centered around 1030 nm. The backward wave generated at 2712 nm at room temperature, but the output could be tuned by 3 nm by changing the temperature of the PPKTP crystal, see Figure 7. This corresponds to a tuning rate of -1.77 GHz/K. The linewidth was as narrow as 43 pm, or 1.75 GHz, with a temporal stability of 65 MHz, and it was obtained without any active means of stabilization. The beam was launched a distance of 2.9 m in the laboratory and the air transmission was measured while the wavelength was scanned, see red graph in Figure 7. At 2.7 μm there is a partial overlap between CO_2 and H_2O absorption lines, while other trace gases could be neglected. By using the HITRAN data base a concentration of 410 ppm of CO_2 and 17.5% relative humidity could be deduced. The simulated absorption curve for these concentrations representing a best fit and can be seen as the blue curve in Figure 7.

These findings underscore the potential of BWOPOs as a simple and robust platform for future differential

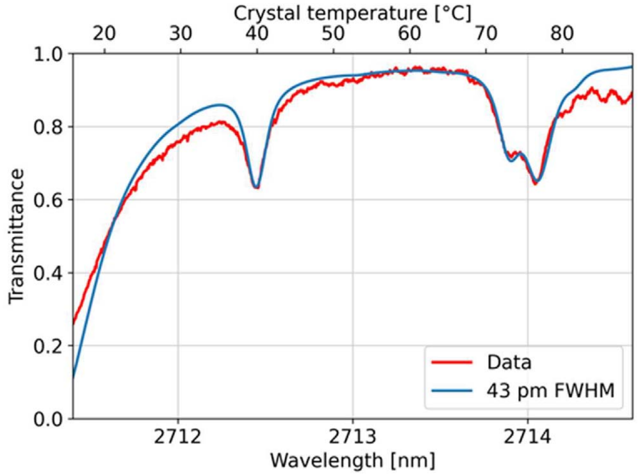

Fig. 7. BWOPO scan measuring ambient air in the laboratory where the two dips in the spectrum comes from absorption of CO_2 and H_2O [44].

absorption lidar (DIAL) systems. The system stability and narrow linewidth provides means for improves detection sensitivity for CO_2 or other trace gases, even for low-concentration scenarios.

5 Summary and future outlook

BWOPOs are highly efficient, energy-scalable devices with a simple architecture that eliminates the need for mirrors or external feedback. The unique distributed feedback mechanism and stability ensures robust operation, even in demanding environments. This feature is particularly valuable for applications where external feedback systems may introduce complexity or alignment challenges.

Moreover, their spectral properties, particularly the narrow linewidth and tunability make them ideal for precision tasks, as the backward wave at the same time is both highly stable and resistant to environmental fluctuations. These advantages underscore the growing interest in BWOPOs across various scientific disciplines and will make them indispensable in applications ranging from biomedical research and quantum optics to different types of spectroscopies like Raman, OCT, or DIAL. Fundamental research will benefit from their use in atomic and molecular physics, cold atom experiments, and nonlinear optics, while industrial applications include precise manufacturing, advanced sensing, and semiconductor inspection. These versatile light sources will help to transform industries, providing unparalleled accuracy and reliability for cutting-edge innovations.

Looking ahead, the integration of BWOPOs with emerging technologies, such as machine learning and adaptive optics, holds promise for unlocking new functionalities and applications. These advancements could pave the way for breakthroughs in fields as diverse as healthcare, environmental monitoring, and fundamental physics. Future research aims to demonstrate continuous wave devices and further enhance their energy efficiency, extend wavelength coverage, and explore new material systems for broader applicability.

Funding

Funding has been provided by the Swedish Foundation for Strategic Research grant no. STP19-0081 and the Swedish Research Council grants 2019-04330 and 2024-05529.

Conflicts of interest

The authors have no conflict of interest.

Data availability statement

This article has no associated data generated.

Author contribution statement

Both authors have contributed to and reviewed the manuscript.

References

1 Dunn MH, Ebrahimzadeh M, Parametric generation of tunable light from continuous wave to femtosecond pulses, *Science* **286**, 1513 (1999). https://doi.org/10.1126/science.286.5444.1513.
2 Byer R, Piskarskas A, Feature issue on optical parametric oscillation and amplification, *J. Opt. Soc. Am. B* **9**, 1656 (1993). https://doi.org/10.1364/JOSAB.10.001656.
3 Myers LE, Eckardt RC, Fejer MM, Byer RL, Bosenberg WR, Pierce JW, Quasi-phase-matched 1.064-μm-pumped optical parametric oscillator in bulk periodically poled $LiNbO_3$, *Opt. Lett.* **20**, 52 (1995). https://doi.org/10.1364/OL.20.000052.
4 Armstrong JA, Bloembergen N, Ducuing J, Pershan PS, Interactions between light waves in a nonlinear dielectric, *Phys. Rev.* **127**, 1918 (1962). https://doi.org/10.1103/PhysRev.127.1918.
5 Giordmaine J, Miller R, Tunable coherent parametric oscillation in $LiNbO_3$ at optical frequencies, *Phys. Rev. Lett.* **14**, 973 (1965). https://doi.org/10.1103/PhysRevLett.14.973.
6 Akhmanov SA, Kovrigin A, Piskarskas A, Fadeev V, Khokhlov R, Observation of parametric amplification in the optical range, *JETP Lett.* **2**, 191 (1965).
7 Johnson HR, Backward-wave oscillators, *Proc. IRE* **43**, 684 (1955). https://doi.org/10.1109/JRPROC.1955.278054.
8 Harris SE, Proposed backward wave oscillation in the infrared, *Appl. Phys. Lett.* **9**, 114 (1966). https://doi.org/10.1063/1.1754668.
9 Canalias C, Pasiskevicius V, Mirrorless optical parametric oscillator, *Nat. Photonics* **1**, 459 (2007). https://doi.org/10.1038/nphoton.2007.137.
10 Ding YJ, Khurgin JB, Backward optical parametric oscillators and amplifiers, *IEEE J. Quantum Electron.* **32**, 1574 (1996). https://doi.org/10.1109/3.535361.
11 Webjörn J, Laurell F, Arvidsson G, Blue light generated by frequency doubling of laser diode light in a lithium niobate channel waveguide, *IEEE Photonics Technol. Lett.* **1**, 316 (1989). https://doi.org/10.1109/68.43360.
12 Lim EJ, Fejer MM, Byer RL, Second harmonic generation of green light in a periodically-poled planar lithium niobate waveguide, *Electron. Lett.* **25**, 174 (1989). https://doi.org/10.1049/el:19890495.
13 Van der Poel CJ, Bierlein JD, Brown JB, Colak S, Efficient type I blue second-harmonic generation in periodically segmented $KTiOPO_4$ waveguides, *Appl. Phys. Lett.* **57**, 2074 (1990). https://doi.org/10.1063/1.103945.

14 Laurell F, Brown JB, Bierlein JD, Sum-frequency generation in segmented KTP waveguides, *Appl. Phys. Lett.* **60**, 1064 (1992). https://doi.org/10.1063/1.106445.

15 Yamada M, Nada N, Saitoh M, Watanabe K, First-order quasi-phase matched $LiNbO_3$ waveguide periodically poled by applying an external field for efficient blue second-harmonic generation, *Appl. Phys. Lett.* **62**, 435 (1993). https://doi.org/10.1063/1.108925.

16 Karlsson H, Laurell F, Electric field poling of flux grown $KTiOPO_4$, *Appl. Phys Letts.* **71**, 3474 (1997). https://doi.org/10.1063/1.120363.

17 Hirohashi J, Pasiskevicius V, Wang S, Laurell F, Picosecond blue light-induced absorption in single-domain and periodically poled ferroelectrics, *J. Appl. Phys.* **101**, 033105 (2007). https://doi.org/10.1063/1.2434007.

18 Tjörnhammar S, Maestroni V, Zukauskas A, Uždavinys TK, Canalias C, Laurell F, Pasiskevicius V, Infrared absorption in KTP isomorphs induced with blue picosecond pulses, *Opt. Mater. Express* **5**, 2951 (2015). https://doi.org/10.1364/OME.5.002951.

19 Hansson G, Karlsson H, Wang S, Laurell F, Transmission measurements in KTP and isomorphic compounds, *Appl. Opt.* **39**, 5058 (2000). https://doi.org/10.1364/AO.39.005058.

20 Vanherzeele H, Bierlein JD, Magnitude of the nonlinear-optical coefficients of $KTiOPO_4$, *Opt. Lett.* **17**, 982 (1992). https://doi.org/10.1364/OL.17.000982.

21 Zukauskas A, Strömqvist G, Pasiskevicius V, Laurell F, Fokine M, Canalias C, Fabrication of submicrometer quasi-phase-matched devices in KTP and RKTP, *Opt. Mater. Express* **1**, 1319 (2011). https://doi.org/10.1364/OME.1.001319.

22 Liljestrand C, Laurell F, Canalias C, Periodic poling of Rb-doped $KTiOPO_4$ by coercive field engineering, *Opt. Expr.* **24**, 14682 (2016). https://doi.org/10.1364/OE.24.014682.

23 Mutter P, Zukauskas A, Canalias C, Domain dynamics in coercive-field engineered sub-μm periodically poled Rb-doped $KTiOPO_4$, *Opt. Mater. Expr.* **12**, 4332 (2022). https://doi.org/10.1364/OME.467806.

24 Coetzee RS, Zukauskas A, Canalias C, Pasiskevicius V, Low-threshold, mid-infrared backward-wave parametric oscillator with periodically poled Rb:KTP, *APL Photonics* **3**, 071302 (2018). https://doi.org/10.1063/1.503549.

25 Kneller J, Flannigan L, Xu C-Q, Design considerations for continuous wave intracavity backwards optical parametric oscillators, *Photonics* **11**, 318 (2024). https://doi.org/10.3390/photonics11040318.

26 Godard A, et al., Backward optical parametric oscillator threshold and linewidth studies, *J. Opt. Soc. Am. B* **39**, 408 (2022). https://doi.org/10.1364/JOSAB.445246.

27 Strömqvist G, Pasiskevicius V, Canalias C, Montes C, Coherent phase-modulation transfer in counterpropagating parametric down-conversion, *Phys. Rev. A* **84**, 023825 (2011). https://doi.org/10.1103/PhysRevA.84.023825.

28 Liljestrand C, Zukauskas A, Pasiskevicius V, Canalias C, Highly efficient mirrorless optical parametric oscillator pumped by nanosecond pulses, *Opt. Lett.* **42**, 2435 (2017). https://doi.org/10.1364/OL.42.002435.

29 Mølster KM, Guionie M, Mutter P, Zheng A, Dherbecourt J-B, Melkonian J-M, Délen X, Zukauskas A, Laurell F, Georges P, Raybaut M, Godard A, Pasiskevicius V, Highly efficient, high average power, narrowband, pump-tunable BWOPO, *Opt. Lett.* **48**, 6484 (2023). https://doi.org/10.1364/OL.506647.

30 Mølster KM, Negri R, Zukauskas A, Lee CSL, Laurell F, Pasiskevicius V, Multi-transversal mode pumping of narrow-bandwidth backward wave optical parametric oscillator, *Opt. Express* **31**, 24320 (2023). https://doi.org/10.1364/OE.494059.

31 Zukauskas A, Viotti A-L, Liljestrand C, Pasiskevicius V, Canalias C, Cascaded counter-propagating nonlinear interactions in highly-efficient sub-μm periodically poled crystals, *Sci. Rep.* **7**, 1 (2017). https://doi.org/10.1038/s41598-017-07016-y.

32 Mutter P, Zukauskas A, Viotti A-L, Canalias C, Pasiskevicius V, Phase-locked degenerate backward wave optical parametric oscillator, *APL Photonics* **8**, 026104 (2023). https://doi.org/10.1063/5.0135589.

33 Mutter P, Laurell F, Pasiskevicius V, Zukauskas A, Backward wave optical parametric oscillation in a waveguide, *npj Nanophoton.* **1**, 38 (2024). https://doi.org/10.1038/s44310-024-00042-5.

34 Calil Kores C, Canalias C, Laurell F, Quasi-phase matching waveguides on lithium niobate and KTP for nonlinear frequency conversion: a comparison, *APL Photonics* **6**, 091102 (2021). https://doi.org/10.1063/5.0060096.

35 Volk MF, Rüter CE, Kip D, Rb/Ba side-diffused ridge waveguides in KTP, *Opt. Express* **25**, 19872 (2017). https://doi.org/10.1364/OE.25.019872.

36 Jang H, Viotti A-L, Strömqvist G, Zukauskas A, Canalias C, Pasiskevicius V, Counter-propagating parametric interaction with phonon-polaritons in periodically poled $KTiOPO_4$, *Opt. Express* **25**, 2677 (2017). https://doi.org/10.1364/OE.25.002677.

37 Brackett CA, Dense wavelength division multiplexing networks: principles and applications, *IEEE J. Sel. Areas Commun.* **8**, 948 (1990). https://doi.org/10.1109/49.57798.

38 Li G, Recent advances in coherent optical communication, *Adv. Opt. Photon.* **1**, 279 (2009). https://doi.org/10.1364/AOP.1.000279.

39 Christ A, Eckstein A, Mosley PJ, Silberhorn C, Pure single photon generation by type-I PDC with backward-wave amplification, *Opt. Express* **17**, 3441 (2009). https://doi.org/10.1364/OE.17.003441.

40 Gatti A, Corti T, Brambilla E, Temporal coherence and correlation of counterpropagating twin photons, *Phys. Rev. A* **92**, 053809 (2015). https://doi.org/10.1103/PhysRevA.92.053809.

41 Gatti A, Brambilla E, Heralding pure single photons: A comparison between counterpropagating and copropagating twin photons, *Phys. Rev. A* **97**, 013838 (2018). https://doi.org/10.1103/PhysRevA.97.013838.

42 Coetzee RS, Duzellier S, Dherbecourt JB, Zukauskas A, Raybaut M, Pasiskevicius V, Gamma irradiation-induced absorption in single-domain and periodically-poled $KTiOPO_4$ and Rb:$KTiOPO_4$, *Opt. Mater. Express* **7**, 4138 (2017). https://doi.org/10.1364/OME.7.004138.

43 Mølster KM, Duzellier S, Zukauskas A, Lee C, Laurell F, Raybaut M, Pasiskevicius V, Proton irradiation hardness of periodically poled Rb:KTP for spaceborne parametric frequency converters, *Opt. Mater. Express* **13**, 436 (2023). https://doi.org/10.1364/OME.475442.

44 Vågberg A, Brunzell M, Widarsson M, Mutter P, Zukauskas A, Laurell F, Pasiskevicius V, 2.7 μm backward wave optical parametric oscillator source for CO_2 spectroscopy, *Opt. Lett.* **49**, 4553 (2024). https://doi.org/10.1364/OL.531038.